Journal Name

CrystEngComm

Dynamic Article Links ►

Cite this: DOI: 10.1039/c0xx00000x

www.rsc.org/xxxxxx

ARTICLE TYPE

Synthesis of niobium oxide nanowires by polyethylenimine as template at varying pH values

Zhenwei Zhang[a], Geng Zhang[b], Lin He[b], Long Sun[b], Xingmao Jiang[b], Zhi Yun[a]**

Received (in XXX, XXX) Xth XXXXXXXXX 20XX, Accepted Xth XXXXXXXXX 20XX

DOI: 10.1039/b000000x

Nb_2O_5 nanowires were synthesized by hydrothermal method using PEI (polyethylenimine) as the soft template. Study results indicated that, pH value greatly affected Nb_2O_5 nanowires. At high pH (pH=9), worm-like Nb_2O_5 nanomaterials was produced on account of writhing and coiling of chains of PEI. In contrast, Nb_2O_5 nanowires were formed when the pH value was lower than 7, because PEI chains expanded due to electrostatic repulsion between ammonium cations, With the decrease of the pH value, the aspect ratio of Nb_2O_5 nanowires became lower, and the BET surface area was increased. When the pH value reached 1-2, Nb_2O_5 nanowires got a surface area as high as 245 m^2g^{-1}. In dehydrogenation of D-xylose to furfural, the catalysts, Nb_2O_5 nanowires prepared at pH=1-2 and calcined at 500°C showed a high conversion rate and yield, 90.3% and 73.7% respectively.

Controlling the shape of nanocrystals is a hot issue in the last several years. The capping agents play a crucial role in controlling the morphology of metal nanoparticles. For example, poly(vinyl pyrrolidone)(PVP)[1] or Br^{-2} can be used to produce nanocubes. But nanoplates[3] can be formed by sodium citrate (Na_3CA). Morphology of copper[4], gold[5], platinum[6] and other metal nanocrystals are controlled by the same method. Above all, coordination interaction between coordinates (ions or organic molecule) and metal atoms affect largely on morphology of the metal nanocrystals.

The method to control the shape of metal oxides or semiconductors is similar to the metal nanoctrystals. Nowadays, researchers have synthesis huge number of metal oxides: zero-dimensional (0D) like isotropic spheres, cubes, and polyhedrons. 1D like rods and wires, 2D discs and plates[7]. In the process of preparation, one important and effective method is template assembly. Polymers provide an excellent template for synthesizing the metal oxides nanocrystals[8], especially some order mesoporous metal oxides[9]. Polymers can form different shapes of the micelles in various solvents by interacting with the solvent moleculars, different types of nanomaterials can be synthesized[10].

Niobium oxide is a promising catalyst materials, and $Nb_2O_5{\cdot}nH_2O$ which is usually called niobic acid can be used as a solid acid to catalysis many reactions[11]. $Nb_2O_5{\cdot}nH_2O$ plays a good role in conversion of glucose into 5-(hydroxy-methyl)furfural[12]. Moreover catalyst activity of Nb_2O_5 nanorods are better than Nb_2O_5 nanospheres[13]. Single-crystalline Nb_2O_5 nanorods are synthesized by CVD (chemical vapor deposition) methods[14], monoclinic niobium pentoxide nanorods (N-Nb_2O_5) were produced under a high temperature 950℃, this material shows a good properties in humidity detection. So control the shape of Nb_2O_5 can improve the catalyst properties.

In recent works, different methods prepared diverse shapes of Nb_2O_5, including different niobium precursors and templates. Using $NbCl_5$ as the precursor and copolymer as the template, a wormlike mesoporous Nb_2O_5 nanomaterial is obtained[15], however, $NbCl_5$ is expensive and more active than other niobium salts. Layered HNb_3O_8 was prepared by exfoliated bulk Nb_2O_5 using tetra(n-butylammonium) hydroxide[16]. The hydrothermal treatment of a niobium peroxo complex can obtain Nb_2O_5 with high surface but low crystallinity[17]. High surface area mesoporous niobium oxides were prepared using amphiphilic block copolymers (Pluronic P123 and P85)[18], cubic pores and hexagon pores[19] can be formed in mesoporous Nb_2O_5 by adding little amount of NaCl solution and controlling the evaporation rate of the solvent. In addition, Nb_2O_5 nanorods can be synthesized by applying trioctylamine as the template[13].

In this work, we firstly made use of polyethylenimine(PEI) as the template to synthesize the Nb_2O_5 nanowires and wormlike nanomaterials. PEI is a polymer with repeating unit composed of an amine group and two-carbon chain. The structure of this polymer differs from other polymers for its structure, in a previous work, Chandan Kumar[20] and collaborators calculated the molecular skeleton by utilizing chemical software. In the molecular dynamics study, they concluded that the PEI polymer is highly coiled at high pH value (basic medium), while the chains elongated at low pH value (strong acidic conditions). This simulated result was consistent with the experimental result in the literature[21]. We firstly used this experimental phenomenon to control the shape of niobium oxides by the structures of PEI under different pH value.

Furfural is a widely used chemical intermediate to produce value compounds[22]. Xylose is the most abundant precursor to synthesize furfural[23]. In industrial process, liquid acid (e.g., sulfuric acid or phosphoric acid) was used as the catalyst, which brought many problems such as high toxicity, high corrosity, and environmental harm[24]. Developing solid acid can solve these problems. Nb_2O_5 is a water tolerant solid acid[25] suitable for this reaction[26]. In this paper, the reaction of xylose to furfural was carried out to test the activity of the Nb_2O_5 nanomaterials.

Synthesis process of the Nb_2O_5 nanomaterials can be seen in Electronic Supplementary Information. The synthesis of Nb_2O_5 nanowires were carried out in acid conditions. HNO_3 was used to tuned pH value of the solution to 1-2(High acidity), 4-5(Medium acidity), 6-7(Low acidity) respectively. A yellow or black gel was formed (see photographs in SI), after series treatment, a powder can be obtained. Which was named as NN-180-H, NN-180-M, NN-180-L for the sample synthesized at high acidic, medium acidic and low acidic conditions, respectively. In order to remove the remaining PEI in the as-prepared samples, NN-180-H, NN-180-M and NN-180-L were treated at 500°C in air for 6h, and a white powder obtained was denoted as NN-500-H, NN-500-M and NN-500-L, respectively.

The synthesis of Nb_2O_5 wormlike nanometrial is similar to that of nanowires except that the pH value was tuned to 9-10 by $NH_3 \cdot H_2O$. The white powder we got was named as NW-180. After heat treatment at 500°C in air for 6h, the sample produced was denoted as NW-500. Characterization details of Nb_2O_5 nanomaterials were seen in SI

Ammonium niobium oxalate was hydrothermal treatment at 180℃ for 72 h, fig. 1(a) and (b) shows two types of Nb_2O_5 were formed under acid and base condition. In the acid condition, PEI chain stretch to the linear shape in fig. 1(a), Nb_2O_5 nanowires were formed along the linear chain. In the base condition, Nb_2O_5 nanowires were highly curved to wormlike nanomaterials in fig. 1(b) because of the curved chain of PEI as the soft template.

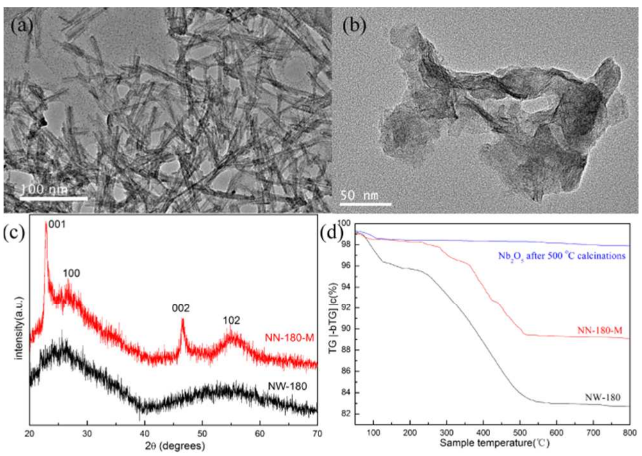

Fig. 1 Morphology of Nb_2O_5 nanomaterials, XRD data and TG data of NN-180-M, NW-180

X-ray diffraction data was shown in Fig. 1(c), NN-180-M is Nb_2O_5 nanowires, 2θ values of planes 22.6, 28.3, 46.1, and 55.2 can be indexed as the (001), (100), (002) and (102) crystal planes of Nb_2O_5 nanowires according to the standard card (JCPDS No. 18-0911). Compared with NN-180-M, crystal plane of Nb_2O_5 prepared in base condition is not so obvious, but the peak shape of NW-180 coincides with the reference[15]. Fig. 1(d) show that there is little amount of PEI adhering on the Nb_2O_5 surface about 8.3% in NN-180-M and 15.2% in NW-180 respectively and after 500℃ little changes can be observed on TG curves showing the PEI all removed comparing with the calcined sample.

Further research showed that the acidity influenced the aspect ratio of Nb_2O_5 nanowires significantly. The average aspect ratio of the nanowires synthesized at high acidity (NN-180-H) was about 4.11 (Fig. 2a and 2d). Lowering the acidity of solution condition will produce longer Nb_2O_5 nanowires. The average aspect ratio of NN-180-M prepared at medium acidity is 8.04 (Fig. 2b and 2d), while longer nanowires (aspect ratio 22.4) were obtained for NN-180-L which was synthesized at low acidity (Fig. 2c and 2d). It was considered that higher acidity gave rise to rapider decomposing rate of ammonium niobium oxalate, resulting in more Nb_2O_5 crystal seeds, which was in favor of forming shorter Nb_2O_5 nanowires. HRTEM analysis the crystal plane information of NN-180-L, in fig. 2(e) hydrothermal treatment under 180℃ get a low crystallinity, but the nanowires is grown along the (001) crystal orientation, interplanar distance is 0.3986 nm accordance with the *d* value 3.9277Å from XRD data.

XRD data shows these three samples in fig. 2(f). From pH value 1-2 to 6-7, (001), (002) crystal plane give obvious peaks, (001), (002) peaks of NN-180-L higher than NN-180-M and NN-180-H shows longer length of the nanowires.

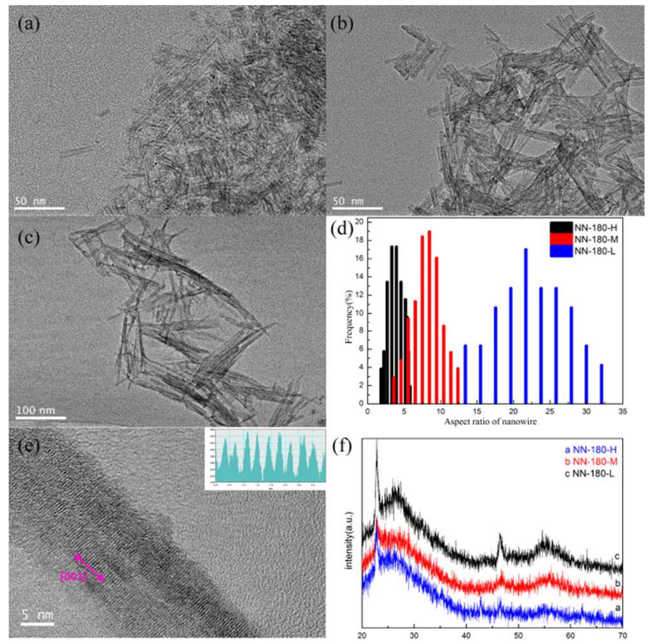

Fig. 2 TEM images of (a) NN-180-H, (b) NN-180-M and (c) NN-180-L; (d) the average length of nanowires for the three samples; (e) HRTEM image of NN-180-L; (d) XRD patterns of the three samples.

NN-180-M and NW-180 were treated in a tube furnace under the temperature 500℃ for 6h. Morphology of NN-180-M is changed to NN-500-M in fig. 3(a), linear shape like Nb_2O_5 becomes high crystallinity, crystals grow up to longer nanowires but NW-500 is still wormlike in fig. 3(b). The crystal type of Nb_2O_5 is transformed to TT-Nb_2O_5(pseudo-hexagonal)[27] (JCPDS No.30-0873). This can also find out from XRD data in fig. 3(d), crystal plane(100), (111), (110) of the Nb_2O_5 have the weak peaks in NN-500-M, but in NW-500 (100), (111), (110) peak strength is higher showing different shape compared to NN-500-M. Further structural analyses of NN-500-M was shown in Fig. 3(c), HRTEM image the crystal plane of NN-500-M, in Fig. 3(d), crystal lines clearly indicate the (001) crystal plane, interplanar distance is about 0.3956 nm accordance with the *d* value 3.9208Å from XRD data. Fast Fourier Transform (FFT) also confirm the wire shape, which was grown along the (001) plane. The width of the wire is about 8 nm.

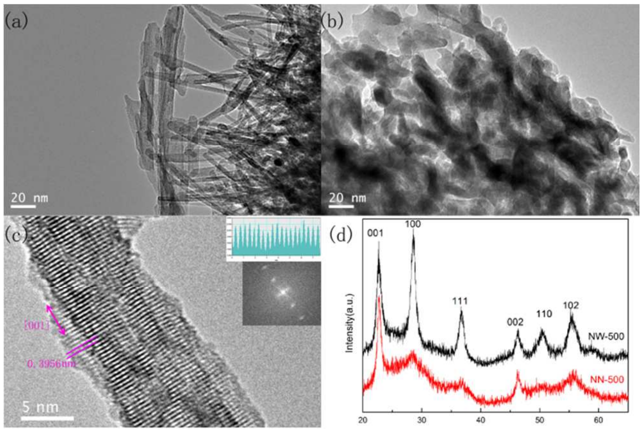

Fig. 3 TEM images of (a) NN-500-M, (b) NW-500. (c) HR-TEM image and FFT of NN-500-M (d) XRD patterns of NN-500-M and NW-500

Nb_2O_5 as the promising catalysts applied in many reactions, so expanding its area can improve its catalysis properties. We determine the BET specific surface area of NN-180-H, NN-180-M, NN-180-L and NW-180. Especially sample NN-180-H, we can get more than 240 m^2g^{-1}, table 1 show BET value of different samples. From the table we can find out that NN-180-H owns a high surface for its small crystal size, and when the pH value higher, surface area decreased. Nb_2O_5 nanowires calcined under the temperature 500℃, surface area reduced. NW-180 owns a low surface area 117 m^2g^{-1}, and after calcined in high temperature, surface area reduced to 85 m^2g^{-1}. Fig. 4(a) shows the N_2-gas adsorption-desorption isotherm and pore size distribution of NN-180-H, The Brunauer-Emmett-Teller (BET) surface area was estimated about 245 m^2g^{-1} for NN-180-H, The Type H4 loop is often associated with narrow slit-like pores[28] and size distribution in fig. 4(b) is wide, these data can also confirm wire like shapes in Nb_2O_5.

Tab. 1 The BET specific surface area of different samples

Sample name	S_{BET}(m^2 g^{-1})	Sample name	S_{BET}(m^2 g^{-1})
NN-180-H	245	NW-180	117
NN-180-M	227	NW-500	85
NN-180-L	212		
NN-500-H	181		
NN-500-M	154		
NN-500-L	130		

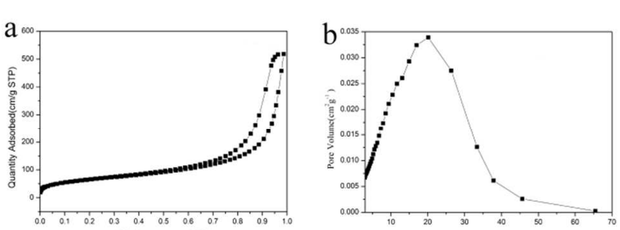

Fig. 4 (a) N_2-gas adsorption-desorption isotherm and (b) pore size distribution of NN-180-H

Tab. 2 Conversion and yield of dehydrogenation of xylose to furfural by Nb_2O_5

Sample name	Conversion/%	Yield/%
NN-180-H	9.8	3.2
NN-180-M	8.3	2.4
NN-180-L	8.4	1.9
NN-500-H	90.3	73.7
NN-500-M	88.5	60.6
NN-500-L	83.6	64.4
NW-180	8.1	1.2
NW-500	30.5	20.9

Reaction condition：20ml DMSO; catalyst 0.01 g; xylose 0.1 g; 120; 2h

According to the reference[29], we chose DMSO as the solvent, reaction temperature 120℃, reaction time 2 h. Tab. 2 shows the activity of the Nb_2O_5. The activity of NN-180-H, NN-180-M, NN-180-L are all very low because of absorbing a small amount of PEI on their surface (fig. 1(d)). After calcined under 500℃ for 6h, PEI was removed and the activity was enhanced, higher surface area Nb_2O_5 prepared in acid condition improve the conversion of xylose and yield of furfural. NN-500-H shows a good conversion and yield about 90.3% and 73.7% respectively. The activity of NW-180 prepared under base condition is the lowest on account of $NH_3{\cdot}H_2O$ and PEI, but NW-500 prepared from NW-180 under 500℃ for 6h increase the acid sites like zeolites removing NH_4^+ ions on its surface and enhanced the activity.

The Nb_2O_5 catalyst property results are good agreement with FT-IR data, in fig. 5(a) (NN-180-M) the band located at 787cm^{-1}can be attribute to v(Nb–O–Nb) vibrations, and 595cm^{-1} is attribute to v(Nb–O) vibration[30]. The band 1627cm^{-1} is due to the bending vibrations of H_2O molecules, and 3409cm^{-1} and 3203 $cm^{-1}$are due to the stretching vibration of OH group, 1403cm^{-1} is the vibration from organic compounds such as PEI which low down the catalyst activity. The IR absorption of NW-180 is similar with NN-180-M except C-N vibration at 1133cm^{-1} on account of more quantity PEI than NN-180-M, this result is good accordance with TG data in fig. 1(d). After calcined the Nb_2O_5, IR spectrum are changed in fig. 5(c) and (d), NN-180-M transfer to NN-500-M by disappearing 1600cm^{-1} peak, however vibration strength of OH group in NN-500-M is stronger than NW-500 under the same temperature treatment displaying the acidity of the NN-500-M nanowires higher than NW-500, so the different activity in dehydrogenation of D-xylose to furfural leading to the different conversion and yield.

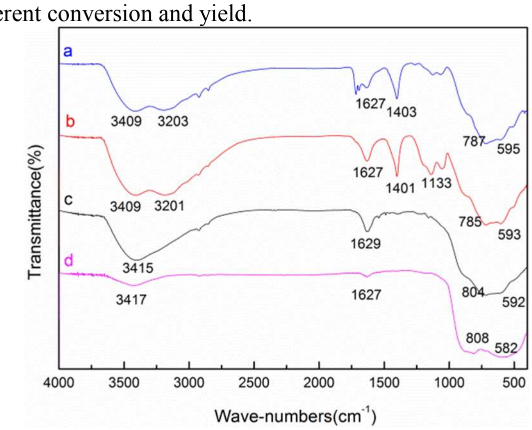

Fig. 5 FT-IR spectra of (a) NN-180-M, (b) NW-180, (c) NN-500-M and (d) NW-500.

In summary, Nb_2O_5 nanomaterial can be synthesized by hydrothermal treatment using PEI as the soft template. The pH value of the reaction system had a significant influence on the aspect ratio of Nb_2O_5 nanowires, wormlike material was obtained under alkalinic conditions. Furthermore, the aspect ratio of the nanowires was decreased with increasing the acidity. After calcination, the nanowire morphology was maintained and the crystallinity was enhanced, the specific area was reduced. As a solid acid catalyst, the calcined Nb_2O_5 nanowires can be used for dehydrogenation of xylose to furfural, and the activity was determined by the surface area and the acidity of the Nb_2O_5 nanowires. The high conversion (90.3%) and yield (73.7%) demonstrated by the calcined Nb_2O_5 nanowires indicate that it is a promising catalyst for the dehydrogenation of xylose to furfural.

Acknowledgements

This work was supported by the Specially Hired Professorship-funding of Jiangsu province No.scz1211400001, the Funding for innovative team of Jiangsu province, and the start-up funds from Changzhou University Jiangsu province, Jiangsu key laboratory of advanced catalytic material and technology, Key laboratory of fine petrochemical engineering and PAPD of Jiangsu Higher Education Institutions.

Project No.21373034 supported by National Natural Science Foundation of China.

Notes and references

[a] *State Key Laboratory of Materials-Oriented Chemical Engineering, College of Chemistry and Chemical Engineering, Nanjing University of Technology, Nanjing 210009, China. Tel./fax: +86 25 83587190.*
E-mail address: qianyangrun@163.com. yunzhi@njut.edu.cn (Z. Yun).
[b]*Key Laboratory of Fine Petrochemical Engineering, Changzhou University, Changzhou 213164, PR China. Fax: +86-519-8 633-0251; Tel: +86-519-8633-0253*
E-mail address: jxm@cczu.edu.cn.

† Electronic Supplementary Information (ESI) available: [details of any supplementary information available should be included here]. See DOI: 10.1039/b000000x/

1. Q. Zhang, W. Li, L.-P. Wen, J. Chen and Y. Xia, *Chem. Eur. J.*, 2010, **16**, 10234-10239.
2. D. Yu and V. W.-W. Yam, *J. Am. Chem. Soc.*, 2004, **126**, 13200-13201.
3. Q. Zhang, N. Li, J. Goebl, Z. Lu and Y. Yin, *J. Am. Chem. Soc.*, 2011, **133**, 18931-18939.
4. M. Jin, G. He, H. Zhang, J. Zeng, Z. Xie and Y. Xia, *Angew. Chem. Int. Ed.*, 2011, **50**, 10560-10564.
5. D. K. Smith and B. A. Korgel, *Langmuir*, 2008, **24**, 644-649.
6. Z.-c. Zhang, J.-f. Hui, Z.-C. Liu, X. Zhang, J. Zhuang and X. Wang, *Langmuir*, 2012, **28**, 14845-14848.
7. Y.-w. Jun, J.-s. Choi and J. Cheon, *Angew. Chem. Int. Ed.*, 2006, **45**, 3414-3439.
8. Y. Mai and A. Eisenberg, *Acc. Chem. Res.*, 2012, **45**, 1657-1666.
9. J. N. Kondo and K. Domen, *Chem. Mater.*, 2007, **20**, 835-847.
10. F. H. Schacher, P. A. Rupar and I. Manners, *Angew. Chem. Int. Ed.*, 2012, **51**, 7898-7921.
11. K. Tanabe, *Catal. Today*, 2003, **78**, 65-77.
12. K. Nakajima, Y. Baba, R. Noma, M. Kitano, J. N. Kondo, S. Hayashi and M. Hara, *J. Am. Chem. Soc.*, 2011, **133**, 4224-4227.
13. Y. Zhao, C. Eley, J. Hu, J. S. Foord, L. Ye, H. He and S. C. E. Tsang, *Angew. Chem. Int. Ed.*, 2012, **51**, 3846-3849.
14. R. Fiz, F. Hernandez-Ramirez, T. Fischer, L. Lopez-Conesa, S. Estrade, F. Peiro and S. Mathur, *J. Phys. Chem. C*, 2013, **117**, 10086-10094.
15. X. Chen, T. Yu, X. Fan, H. Zhang, Z. Li, J. Ye and Z. Zou, *Appl. Surf. Sci.*, 2007, **253**, 8500-8506.
16. A. Takagaki, D. Lu, J. N. Kondo, M. Hara, S. Hayashi and K. Domen, *Chem. Mater.*, 2005, **17**, 2487-2489.
17. E. R. Leite, C. Vila, J. Bettini and E. Longo, *J. Phys. Chem. B*, 2006, **110**, 18088-18090.
18. K. Nakajima, T. Fukui, H. Kato, M. Kitano, J. N. Kondo, S. Hayashi and M. Hara, *Chem. Mater.*, 2010, **22**, 3332-3339.
19. L. Ye, S. Xie, B. Yue, L. Qian, S. Feng, S. C. Tsang, Y. Li and H. He, *CrystEngComm*, 2010, **12**, 344-347.
20. C. K. Choudhury and S. Roy, *Soft Matter*, 2013, **9**, 2269-2281.
21. K. P. Sharma, C. K. Choudhury, S. Srivastava, H. Davis, P. R. Rajamohanan, S. Roy and G. Kumaraswamy, *J. Phys. Chem. B*, 2011, **115**, 9059-9069.
22. R. Karinen, K. Vilonen and M. Niemelä, *ChemSusChem*, 2011, **4**, 1002-1016.
23. A. S. Dias, S. Lima, M. Pillinger and A. A. Valente, *Carbohydr. Res.*, 2006, **341**, 2946-2953.
24. T. Armaroli, G. Busca, C. Carlini, M. Giuttari, A. M. Raspolli Galletti and G. Sbrana, *J. Mol. Catal. A: Chem.*, 2000, **151**, 233-243.
25. C. García-Sancho, I. Sádaba, R. Moreno-Tost, J. Mérida-Robles, J. Santamaría-González, M. López-Granados and P. Maireles-Torres, *ChemSusChem*, 2013, **6**, 635-642.
26. X. Shi, Y. Wu, P. Li, H. Yi, M. Yang and G. Wang, *Carbohydr. Res.*, 2011, **346**, 480-487.
27. R. Brayner and F. Bozon-Verduraz, *Phys. Chem. Chem. Phys.*, 2003, **5**, 1457-1466.
28. K. S. W. S. D. H. E. R. A. W. H. L. M. R. A. P. J. R. T. SIEMIENIEWSKA, *Pure & Appl. Chem.*, 1985, **57**, 603-619.
29. F. Wang, H.-Z. Wu, C.-L. Liu, R.-Z. Yang and W.-S. Dong, *Carbohydr. Res.*, 2013, **368**, 78-83.
30. M. Ristić, S. Popović and S. Musić, *Mater. Lett.*, 2004, **58**, 2658-2663.